AA15 - Online FTIR Analysis for Improved Efficiency in Alumina Production

Jonathon Speed[1] and Stephanie Wood[2]
1. Product and Applications Manager
2. Applications Scientist
Keit Spectrometers, Oxford, United Kingdom
Corresponding author: jonathon.speed@keit.co.uk

Abstract

Online analysis of continuous and batch processes has seen a dramatic increase in recent years, with examples ranging from petrochemicals to pharmaceuticals, to industrial biotechnology and food & drink. The particularly challenging environment of alumina processing has meant that instrumentation needs specific features and characteristics to be truly suitable, features such as robustness, resistance to caustic conditions both in the analyte and the ambient environment, and reliability for long-term continuous use. Here we present the development of a novel FTIR spectrometer that achieves these requirements through the use of a static optics arrangement of mirrors, and a stable diamond-tipped light-pipe probe.

Firstly, we give a very brief explanation of spectroscopic analysis, and the difference between FTIR and other infrared methodologies. Next, we outline the novel arrangement of mirrors required to produce an interferogram without moving mirrors and compare the benefits and drawbacks of this approach with those of conventional designs.

We then share the results of laboratory analysis of synthetic Bayer liquors, with detection limits for aluminium hydroxide, sodium hydroxide, sodium carbonate and various sodium salts of organic acids. We then share the results of analysis on production samples – predominantly from spent liquor lines.

Lastly, we present work on in situ ultrasonic descaling solutions to avoid scale buildup and provide continuous cleaning of the probe – preventing the need for probe removal and manual cleaning.

Keywords: Online analysis, process improvement, FTIR spectroscopy, process analytical technology, real time analysis.

1. Introduction

Online process analytical technology (PAT) is an important area of development in a wide range of industrial processes [1, 2], and a key element of Industry 4.0 – the commonly accepted fourth industrial revolution we are currently experiencing. Traditional instrumentation (such as pH and temperature probes) is being complimented with more advanced techniques such as spectroscopy.

Spectroscopy can be defined as the interaction of light with matter, and the wavelength and energy of the light absorbed determines the underlying interaction studied. A full explanation of all the different spectroscopic techniques and wavelengths is beyond the scope of this article and is available elsewhere [3]. The majority of PAT implementations make use of vibrational spectroscopy – namely near-infrared (NIR), Raman and mid-infrared Fourier transform (FTIR) spectroscopies.

1.1 Near-Infrared Spectroscopy

NIR spectroscopy [4] is an absorbance technique where light in the wavelength range 0.8 – 2 μm is used to irradiate a sample and the light absorbed is proportional to combination and overtone bands of fundamental infrared vibrations. NIR instruments can be built on either dispersive (i.e. gratings and prisms) or Fourier transform (i.e. Michelson interferometers) principles. In either case the instrument is typically positioned far away from the sampling point, using a near infrared fibre to transmit the light from the source to the sample and back to the detector. To date most PAT spectrometers installs involve NIR instruments, because they have a track record of reliability in challenging environments. However, calibration and maintenance of NIR based approaches is "a complex process, requiring long-term database maintenance and calibration model update" [5]. Moreover, the lack of chemical information from NIR spectroscopy as a technique makes identifying and differentiating similar molecular structures with NIR a challenge at best, and impossible at worst.

1.2 Mid-Infrared FTIR Spectroscopy

FTIR spectroscopy [6] is also an absorbance technique, one which uses light between 2 and 20 μm, but it can offer substantially more information than NIR, as it investigates the fundamental vibrations of molecules rather than overtones and combination bands. This means that small changes in molecular structure can be identified and quantified [7], for example in the differentiation of proteins [8]. Conventional FTIR spectrometers use an arrangement of fixed and moving mirrors (based on the Michelson interferometer [9]), which means the instrument needs to be removed from any sources of vibration – common in industrial processes. While NIR spectrometers can use tried and tested fibres and probes to achieve this with relative ease, FTIR fibres are extremely fragile and have very low through-put of mid-infrared light – making their use in industrial settings very difficult to achieve.

1.3 Raman Spectroscopy

Raman spectroscopy [10] is a scattering and emission technique, where a laser is used to excite the sample to a virtual excited electronic state, which then relaxes back into the ground electronic state. Most molecules relax back into the same state they were initially in, emitting light of the same wavelength used for excitation (Raleigh scattering). A small proportion of molecules relax into a different vibrational state, emitting light that is shifted to a different wavelength (Raman scattering). There are examples of Raman spectroscopy being applied to the study of alumina processing with promising results [11], but in highly controlled environments at the laboratory scale. Raman instruments typically use fibre probes and near infrared lasers (either 785 or 1064 nm wavelengths). Raman spectroscopy often suffers from high fluorescence and requires complicated mathematical processing to remove these artefacts, which can reduce the reliability and robustness of analysis.

Here we present the use of a static optics FTIR spectrometer based on the Sagnac interferometer [12], with no moving parts or fibre optics. This gives the performance of a laboratory FTIR spectrometer but the robustness of a production NIR instrument – greatly increasing the information available for process control and opening the world of real time spectroscopy-based PAT to the alumina processing industry.

2. Instrument Design

We will briefly outline the optical design of conventional instruments and the novel design highlighted here to give context to the stability and performance of the static optics design.

2.1 Conventional FTIR Interferometer Design

Conventional FTIR instruments make use of a Michelson interferometer, as shown in Figure 1. The light is created by a light source (1), such as a silicon carbide infrared emitter. This light is shone onto a beam splitter (2) which sends half the light onto a stationary mirror (3) and the other half onto a moving mirror (4). The light that runs on the stationary path always has the same distance to travel, whilst the path length of the light on the moving mirror changes over time. The light is then recombined at the beam splitter (2) before interacting with the sample and finally landing on a detector (5). The detector is a single pixel of material such as lithium tantalite, deuterated triglycine sulfate or mercury cadmium telluride. The difference in path lengths (caused by the moving mirror) creates an interference pattern that changes over time (as the mirror moves), which creates a changing interference pattern over time. This interference pattern is subjected to a Fourier transform (the "FT" in "FTIR") which ultimately creates a spectrum.

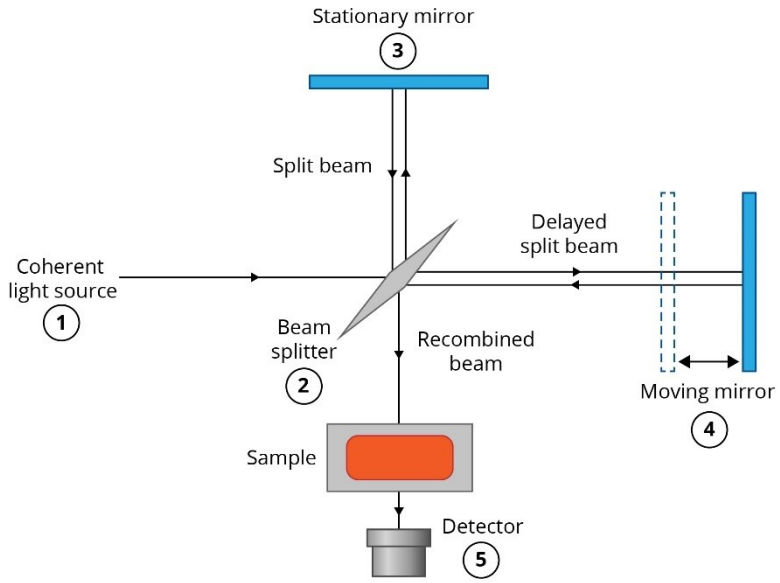

Figure 1. A schematic of a Michelson interferometer showing light path from the light source through the pair of mirrors, the sample and eventually onto a single-pixel detector.

2.2 Static Optics FTIR Interferometer Design

The static optics instrument design outline here makes use of a Sagnac interferometer, as shown in Figure 2. In this instance, the light (from a low powered source) runs through the sample first, before hitting a beam splitter (1). Half the light is reflected to run anti-clockwise through a pair of curved mirrors (2) whilst the other half is transmitted through the beam splitter to run clockwise through the pair of mirrors. Both beams of light are then incident onto a detector array (3) creating an interference pattern with respect to space directly onto the array. This interference pattern is subjected to the same Fourier transform mathematics as conventional designs.

The use of a "Sagnac loop" of mirrors removes the need for moving mirrors and enables the use of secured mirrors onto an industrial baseplate. Ultimately this translates into a design that is significantly more resilient to vibration, as if one aspect of the optical design vibrates then the whole assembly vibrates – resulting in no change in the interference pattern and final spectrum.

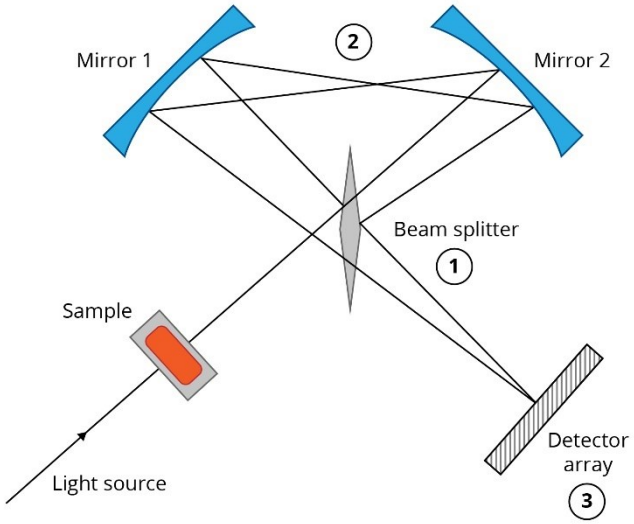

Figure 2. A schematic of the modified Sagnac interferometer showing the light path through the sample, then the "Sagnac loop" before the detector array.

3. Analytical Performance of the Instrument

To establish the performance of the instrument itself for Bayer process analysis, a range of laboratory reference samples was made, and these were used to build a calibration curve using partial least squares (PLS) [13] methodology. Laboratory samples were prepared as follows: stock solutions of 607.5 g/L NaOH, 75 g/L Na_2CO_3 and 155 g/L $Al(OH)_3$ dissolved in 328 g/L NaOH solution. These were mixed and diluted with additional water as appropriate to make a "Design of Experiment" sample set for calibration.

3.1 NaOH, $NaAl(OH)_4$ and Na_2CO_3 Measurements in Spent Liquor

The spectra of these samples are shown below in Figure 3. They have been derivatised to remove baseline offsets present when a sample is heated (infrared spectroscopy is intrinsically linked to heat, so some form of simple pre-treatment is almost always used to remove physical artefacts in the spectrum). A horizontal line has been added for clarity to show where the centre of the derivatized peaks lie. A broad characterization of the spectrum has been performed, with the following assignments: 1660 cm-1: water; 1560 cm-1: sodium carbonate; 1387 cm-1: aluminium hydroxide; 900 – 1100 cm-1: various features from dissolved organic acids and their salts.

The spectra of these samples are shown below in Figure 3. They have been derivatised to remove baseline offsets present when a sample is heated (infrared spectroscopy is intrinsically linked to heat, so some form of simple pre-treatment is almost always used to remove physical artefacts in the spectrum). A horizontal line has been added for clarity to show where the centre of the derivatized peaks lie. A broad characterization of the spectrum has been performed, with the following assignments: 1660 cm-1: water; 1560 cm-1: sodium carbonate; 1387 cm-1: aluminium hydroxide; 900 – 1100 cm-1: various features from dissolved organic acids and their salts.

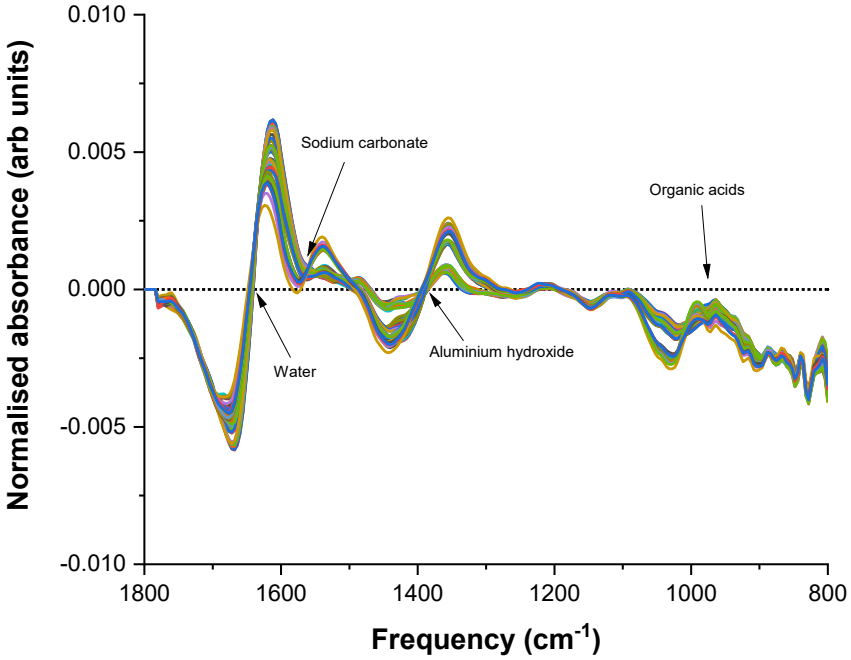

Figure 3. Derivatised spectra of laboratory made and process samples for calibration. Samples were analysed for 120 s at 90 °C on the IRmadilloDiamond spectrometer in a sealed heating cell. A 1st order derivative was performed using a 5-point symmetric Savitzy-Golay smoothing and a 2nd order polynomial.

In each of the quantitative calibrations the process samples were divided into two sets, with some samples being used for model and calibration building, and a subsequent set used for blind prediction to test the model.

The calibration for NaOH is shown below in Figure 4, with a root mean squared error of cross validation (RMSECV) of 7.38 g/L. The RMSECV is the effective average error of the calibration, and can also be used as a limit of detection (LoD) for lower concentration measurements. The measured vs reference values for this calibration show strong linearity, with an R2 of 0.985. The process samples for calibration are all clustered together tightly between 140 and 160 g/L, but are in good agreement with the calibration. The process samples for prediction are in broad agreement with the calibration model, but do show a drift towards over-prediction. The root mean squared error of prediction (RMSEP) of this model is 8.8 g/L, showing substantial promise, but that some optimization is possible.

The calibration for $Al(OH)_3$ (reported as $NaAl(OH)_4$) is shown below in Figure 5. The calibration was built to span a large range of Al, including a zero point with no Al ions present at all (in this case a mixture of NaOH and Na_2CO_3 only). The RMSECV of 4.69 g/L and R^2 of 0.985 shows strong linearity and good average error of the measurement. The RMSEP of this calibration is 5.66 g/L. There is again a slight overprediction of the absolute concentration range, but additional process samples incorporated into this calibration model have a reasonable likelihood of reducing the error and improving the correlation.

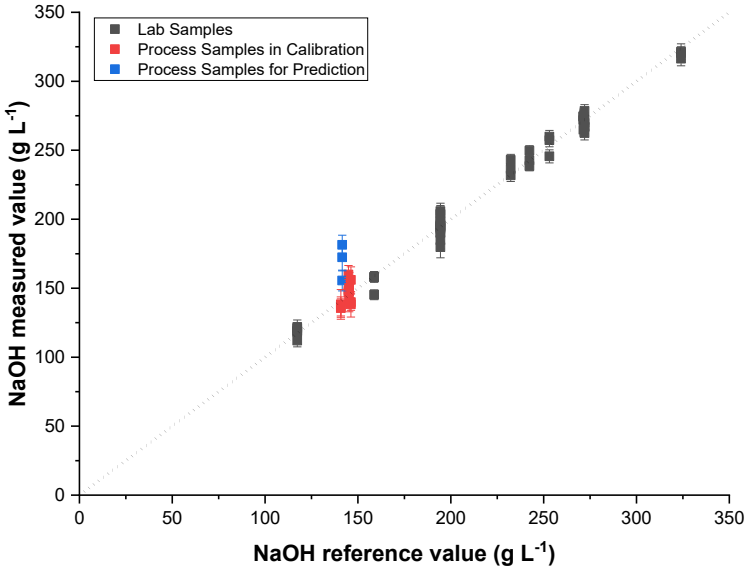

Figure 4. Calibration curve for NaOH built using PLS chemometrics. The RMSECV is 7.38 g/L and R^2 of 0.985.

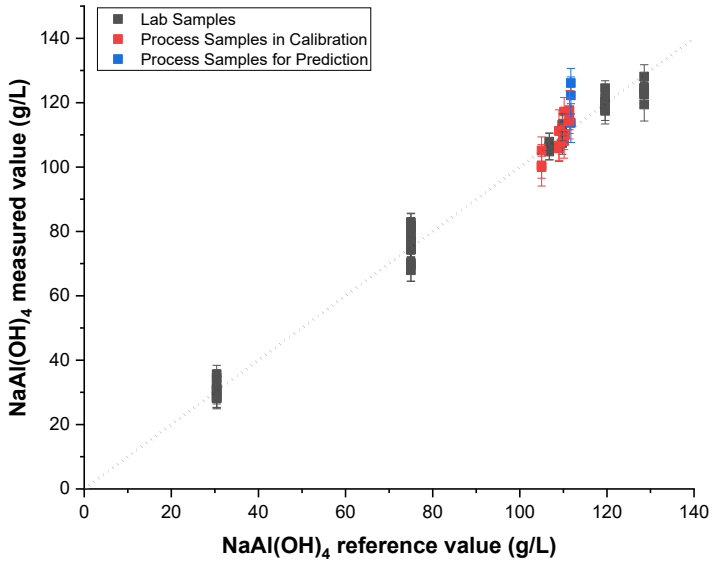

Figure 5. Calibration curve for $NaAl(OH)_4$ built using PLS chemometrics. The RMSECV is 4.69 g/L and R^2 of 0.985.

The calibration for Na_2CO_3 was performed using only laboratory samples because the availability of reference data for process samples was limited. (The laboratory sample reference values were known because samples were made in the laboratory with known amounts of stock solutions.) In this case the results of calibration are presented slightly differently, with measured and reference data shown when available. The measured value alone appears only when reference data is not available as shown in Figure 6.

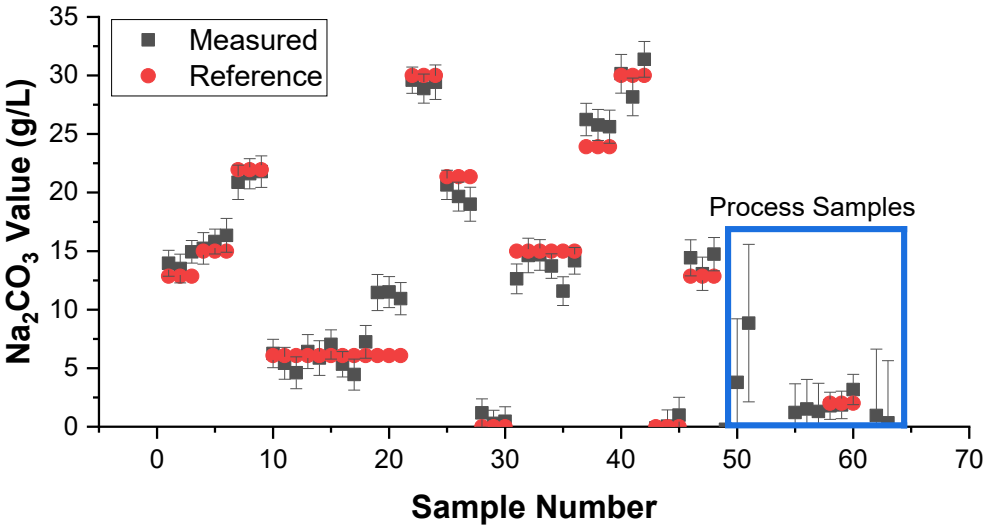

Figure 6. Results for calibration of Na_2CO_3 using laboratory samples and the resulting measurements on process samples with reference data where available.

The resulting RMSECV is 1.36 g/L and an R^2 of 0.982 for the calibration itself, but as this does not contain process samples the results should be considered advisory rather than absolute. The process samples (shown within the blue box in the figure) are in good agreement for samples 55 – 60, but have much large errors for samples 50 – 53, and 60 – 63. This suggests that there are chemicals present within the process samples that are not present in the laboratory samples that must be included in calibration for accurate results. These chemical contaminants are expected, and mostly take the form of organic acids and their sodium salts: most notably oxalate ($Na_2C_2O_4$), formate (HCOONa), acetate (CH_3COONa) and succinate ($C_4H_4Na_2O_4$).

3.2 Organic Acid Salts Measurements

To test the detection limits of organic salts in the calibration a subsequent set of experiments was performed using solely production samples. These were once again measured at 90 °C in a sealed heated cell to prevent evaporation of the water. Chemometric calibrations were performed using support vector regression (SVR) [14] due to a degree of non-linearity in the spectral response. This is assumed to be caused by an interaction between the Al^{3+} ion and the COO^- functionality of the acid salts, the strength of which changes with the concentration of Al and the other acid salts present. A detailed study of this effect is beyond the scope of this paper.

The results for these calibrations have been collated and are shown below in Figure 7. Many of the samples did not contain either sodium formate or sodium succinate, so there are comparatively fewer calibration points for those chemicals. The RMSECV values for sodium oxalate, acetate, formate and succinate are 0.11, 0.26, 0.27 and 0.31 g/L, respectively.

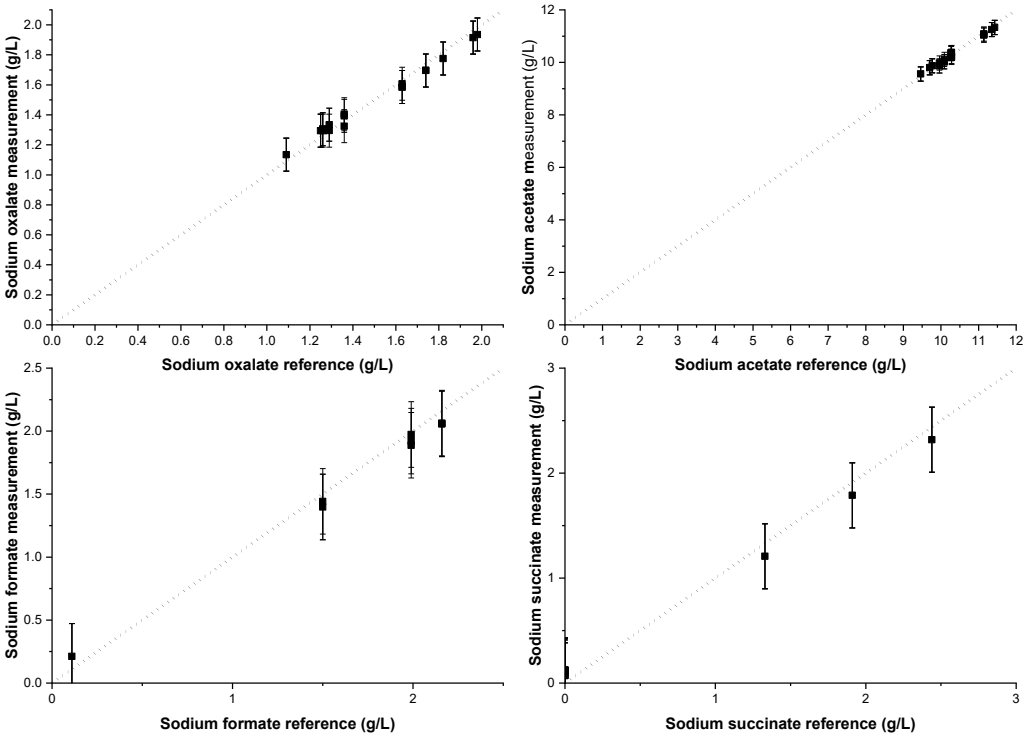

Figure 7. Collated results for sodium salts of organic acid contaminants in process samples. RMSECV values for sodium oxalate, acetate, formate and succinate are 0.11, 0.26, 0.27 and 0.31 g/L respectively.

4. Initial Work on Ultrasonic Cleaning

A key concern in the processing of alumina using the Bayer process is the formation of scale on pipework and the coating of gibbsite minerals onto analytical equipment. Any instrumentation developed for this sector needs to be capable of *in situ* cleaning to become truly effective and enable real time control. A benefit of the static optics design of the spectrometer used in this study is inherent resistance and stability to ultrasonic cleaning. The simplest implementation of ultrasonic cleaning for online measurement is an externally mounted transducer on a process pipe, directly opposite the spectrometer probe. Figure 8 below shows an experimental setup of the spectrometer inserted into a stainless-steel cell with welded port tube to accept the spectrometer, and an externally mounted transducer.

Figure 8. Photograph of the IRmadillo spectrometer installed into a sample cell with gibbsite scaling solution and an externally mounted ultrasonic transducer for descaling experiments.

The cell was filled with saturated $Al(OH)_3$ in NaOH solution at 90 °C and allowed to cool overnight with no stirring. This created a film of gibbsite scale on the surface of the probe. The ultrasonic transducer was activated for 5 s, before a 2 min rest, activated again for 5 s, rested for a further 2 min and activated for a final 5 s. The results of the spectroscopy performed during this time are shown below in Figure 9. Overnight the spectrometer was set to average for 10 s per scan, but during the experiment itself the averaging was reduced to 1 s per scan. This is shown on the figure itself.

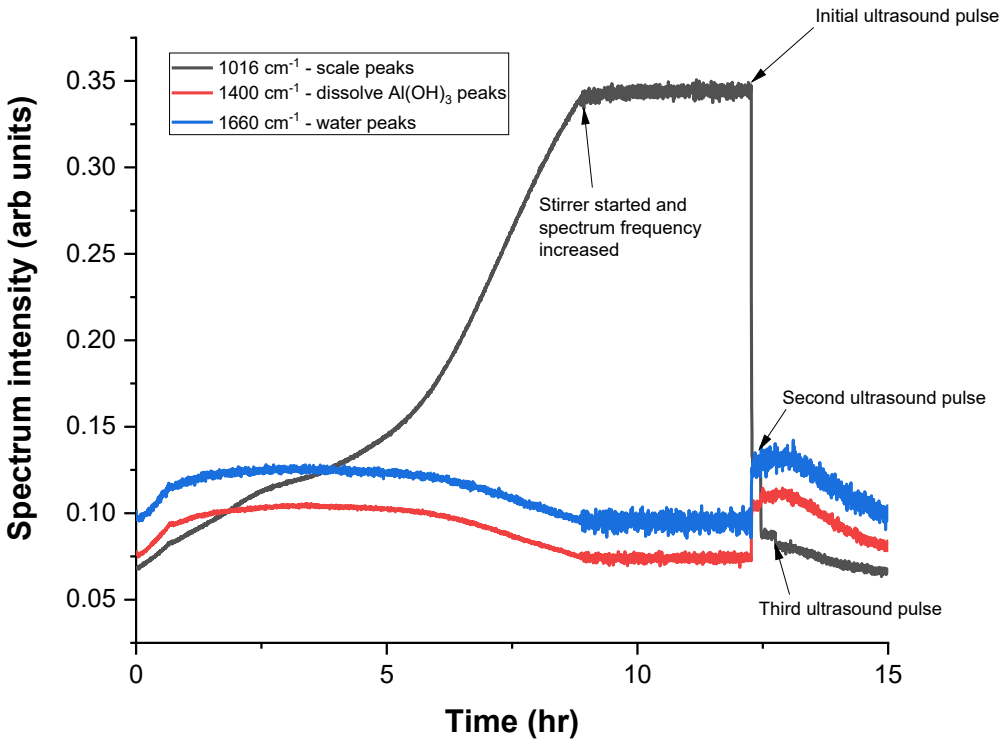

Figure 9. Intensity of peaks for scale (1016 cm^{-1}), dissolved $Al(OH)_3$ (1400 cm^{-1}) and water (1660 cm^{-1}) at various stages throughout the experiment. (The scanning frequency is 10 s overnight and is increased to 1 s frequency during the ultrasound pulsing).

The scale is shown to build up over time, rising from a spectral intensity of 0.7 absorbance units to a maximum of 0.34 over the allotted time (although it should be noted that the rate of growth suggested indefinite scaling without intervention). Over this time the intensity of the dissolved $Al(OH)_3$ and water peaks decreased – showing that the Gibbsite formation blocked the sensing of the liquid analyte of interest. The initial ultrasound pulse removed the substantial majority of the signal from scale almost immediately. Two further pulses removed the scale down to the baseline level of signal. This experiment was designed to represent a worst case scenario with sporadic ultrasonic cleaning, but a more practical periodic ultrasonic pulse of 5 s cleaning every 5 – 10 min of sensing would prevent the formation of any detectable level of scale on the probe itself, ensuring accurate measurements in real world applications.

5. Conclusions and Further Work

The authors conclude that the static optics FTIR spectrometer is sufficiently accurate for the monitoring of alumina processing in the Bayer process, with accurate measurement of $Al(OH)_3$, NaOH, Na_2CO_3 levels enabling real time closed loop control. Furthermore, it is possible to accurately monitor the levels of dissolved organic acid salts with the same instrument, with detection limits of 0.11 – 0.31 g/L depending on species. Lastly, the instrument can be coupled with externally mounted ultrasonic cleaning to ensure scale build up over time does not prevent long term measurement, regardless of the installation location.

The instrument is currently installed in one production site, with early stage discussions with other manufacturing plants world-wide. The authors hope to present more detailed online data from real world installations with potential discussion of return on investment and use case scenarios in due course. This will resolve open questions and concerns about the formation of particles in suspension such as sodium aluminosilicates. The design of the probe is resilient to interference from solids, as an attenuated reflectance probe (ATR) does not rely on traditional reflectance or transmission approaches, and only interacts with approximately 2 μm of liquid – meaning that solids do not interfere with the liquid analysis. It is expected that long term installations in multiple sites with varying impurity levels within the bauxite will resolve this question.

6. References

1. Katherine Bakeev, *Process Analytical Technology*, Oxford, Blackwell Publishing, 2008.
2. W. Chew and P. Sharratt, Trends in process analytical technology, *Analytical Methods*, Vol. 2, No. 10, 2010, 1412-1438.
3. Peter Atkins, *Atkins Physical Chemistry*, 11th Edition, Oxford, Oxford University Press, 2017, 944 pages.
4. Donald A. Burns and Emil W. Ciurczak, *Handbook of Near-Infrared Analysis*, 3rd Edition, Boca Raton, CRC Press, 2007, 834 pages.
5. Nanning Cao, *Calibration optimization and efficiency in near infrared spectroscopy, Graduate Theses and Dissertations,* Iowa State University, 2013, 183 pages.
6. Peter R. Griffiths, James A. De Haseth and James D. Winefordner, *Fourier Transform Infrared Spectroscopy*, Wiley, 2007, 560 pages.
7. George Socrates, *Infrared and Raman characteristic group frequencies,* 3rd Edition, Wiley, 2001.
8. Andreas Bath, Infrared spectroscopy of proteins, *Biochimica et Biophysica Acta (BBA) – Bioenergetics,* Vol. 1767, No. 91, 2007, 1073-1101.
9. A. Michelson and E. Morely, On the relative motion of the Earth and the Luminiferous Ether, *American Journal of Science,* Vol. 34, No. 203, 1887, 333-345.
10. Patrick Hendra, Catherine Jones and Gavin Warnes, *Fourier Transform Raman Spectroscopy,* Ellis Horwood Limited, 1991.

11. W. Rudolph and G. Hefter, Quantitative analysis in alkaline aluminate solutions by Raman spectroscopy, *Analytical Methods,* Vol. 1, No. 2, 2009, 132-138.
12. Georges Sagnac, Regarding the proof for the existence of a luminiferous ether using a rotating interferometer experiment, *Comptes Rendus,* Vol. 157, 1913, 1410-1413.
13. Svante Wold, Michael Sjöström and Lennart Eriksson, PLS regression: A basic tool of chemometrics, *Chemometrics and Intelligents Laboratory Systems,* Vol. 58, No. 2, 2001, 109-130.
14. Alex J. Smola and Bernhard Scholkopf, A tutorial on support vector regression, *NeuroCOLT2 Technical Report Series,* 1998.